Scaling properties of numerical two-dimensional turbulence

A. Babiano,[1] B. Dubrulle,[2,3] and P. Frick[1,4]
[1]*Laboratoire de Meteorologie Dynamique, Ecole Normale Superieure, 24 rue Lhomond, F-75005 Paris, France*
[2]*CNRS, UPR 182, Commissariat à l'Energie Atomique, Service d'Astrophysique, Centre d'Etudes de Saclay, F-91191 Gif sur Yvette, France*
[3]*CNRS, URA 285, Observatoire Midi-Pyrénées, 14 avenue Belin, F-31400 Toulouse, France*
[4]*Institute of Continuous Media Mechanics, Korolyov 1, 614061 Perm, Russia*
(Received 8 November 1994)

We consider two-dimensional (2D) incompressible turbulent flow in a statistically steady state in which energy and enstrophy inputs, localized around a forcing mode, are compensated by a linear frictional force at large scales and viscous dissipation at small scales. The scaling properties of the energy and enstrophy established cascades are studied via the velocity structure functions. The extended self-similarity is used to obtain a better estimate of the scaling exponents of the structure functions at any order. Three distinct scaling regimes are observed. At large scales, corresponding to the inverse cascade of energy, the scaling exponents are well defined and similar to those observed in 3D isotropic turbulence, with large deviations from the Kolmogorov 1941 scaling (strong intermittency). At intermediate scales, where coherent structures dominate, no scaling is present. At small scales, corresponding to the direct enstrophy cascade, a second scaling regime is obtained, with almost nonanomalous scaling exponents (weak intermittency). The intermittency obtained in the two scaling regimes is found to be consistent with the hierarchical intermittency model of turbulence of She and Lévêque [Phys. Rev Lett. **72**, 336 (1994)], developed in the context of 3D turbulence. The model is characterized by two main parameters, Δ and β, describing respectively, the smallest dissipative scales and the degree of intermittency of the energy transfers. These parameters are measured in the two regimes. In the inverse cascade, $\beta=0.7$ and $\Delta=0.47$, close to the values observed in 3D turbulence ($\beta=\Delta=2/3$). In the direct enstrophy cascade, β is close to 1, and Δ close to 0, which explains the weak intermittency observed.

PACS number(s): 47.27.Gs, 47.27.Eq

I. INTRODUCTION

One important characteristic of two-dimensional (2D) turbulence is the presence of strong coherent vortices superposed on a well-mixed background. As shown by Benzi *et al.* [1], these vortices inhibit the cascade locally, and can be viewed as drops of laminar fluids in an other wise turbulent flow. They may bring dominant contributions to energy transfers, which explains the observed dependence of the energy spectrum of 2D turbulence on initial conditions [2,3]. For this reason, it is often considered that, unlike 3D turbulence, 2D turbulence cannot be universal.

Are there any reasons to believe in universality in (2D and 3D) turbulence? In many systems, universality arises from the presence of a group of symmetry, which dictates the shape of the interactions, but not the value of the constants involved. In turbulence, scale invariance is believed to be an important symmetry of the Navier-Stokes equations in both two and three dimensions. It would then be natural to observe some common universal features in 2D and 3D turbulence, independently of the value of the slope of energy spectra. This possibility was recently suggested by Dubrulle [4], who observed that a new model of intermittency in 3D turbulence by She and Lévêque [5] could be interpreted as stemming from a generalized scale covariance principle (see also the interpretation of She and Waymire [6] in terms of infinitely divisible laws). It should therefore be valid in any scale-invariant system apparent to turbulence. This hypothesis has been checked by Frick *et al.* [7] for a class of shell models with different conservation laws. The scale invariance suggested by She-Lévêque with a large spectrum of parameters has been confirmed. The goal of the present contribution is to explore this conjecture by studying the scaling properties of structure functions in a statistically stationary 2D turbulence, and see whether they are compatible with the intermittency model of She and Lévêque (hereafter SL).

The outline of the paper is as follows. After a brief summary of the SL model and its basic hypotheses, and a description of the numerical simulations involved (Sec. II), the scaling properties of the structure functions are studied (Sec. III A). Systematic check of the hypothesis of the SL model is done, and the basic parameters of the model are measured (Secs. III C–III F). A discussion of the results is provided in Sec. IV.

II. THEORETICAL AND NUMERICAL BACKGROUND

A. The hierarchical intermittency model

One interesting property of fully developed 3D turbulence is the existence of a scaling regime in the inertial range for the velocity difference δv_l across a distance l:

$$\langle \delta v_l^p \rangle \sim l^{\zeta_p} . \tag{1}$$

As shown recently by Benzi *et al.* [8], isotropic homogeneous turbulence seems to obey a more general scaling relation, extending property (1) for all l between the energy injection scale to a few Kolmogorov scales:

$$\langle \delta v_l^p \rangle = C_{p,s} \langle \delta v_l^s \rangle^{\zeta_p/\zeta_s} \quad \text{for all } p,s , \tag{2}$$

where $C_{p,s}$ are some numerical constants. This property was called extended self-similarity (hereafter ESS). It enables improved accuracy in the determination of the scaling exponents ζ_p.

The Kolmogorov refined similarity hypothesis predicts that the exponents ζ_p should be related to the corresponding exponent of the energy dissipation ϵ_l over a ball of size l via

$$\zeta_p = \frac{p}{3} + \tau_{p/3} , \tag{3}$$

with

$$\langle \epsilon_l^p \rangle \sim l^{\tau_p} . \tag{4}$$

If the flux of energy was nonintermittent, then all τ_p would be equal to zero, and one would obtain the famous linear scaling $\zeta_p = p/3$ predicted by Kolmogorov in 1941. Direct measurements of the scaling exponents in numerical simulations [9] or in experiments (see, e.g., [10]), however, favor nonzero τ_p. Among the various models proposed to explain this observation, the model of She and Lévêque [5] gives predictions for the ζ_p which fit within 1% the recent improved measured values of Benzi *et al.* [8]. This model was slightly modified by Dubrulle [4] to account for the ESS property, by making use of the "generalized scale" $\langle \delta v_l^3 \rangle / \epsilon_l$ in place of the natural scale l used by She and Lévêque. The corresponding model is then based on three hypotheses concerning the statistical properties of a nondimensional quantity, π_l, defined after the mean energy dissipation ϵ_l:

$$\pi_l = \frac{\epsilon_l}{\epsilon_l^{(\infty)}} , \tag{5}$$

where $\epsilon_l^{(\infty)}$ is a normalization function, which enables us to factorize out all the geometry dependence of the dissipation. That way, π_l truly represents an "inertial range" quantity, independent of external conditions.

The three hypotheses are then as follows.

(i) Similarity:

$$\frac{\delta v_l^3}{\langle \delta v_l^3 \rangle} \overset{\text{scal}}{=} \frac{\epsilon_l}{\langle \epsilon_l \rangle} = \frac{\pi_l}{\langle \pi_l \rangle} , \tag{6}$$

where $\overset{\text{scal}}{=}$ means have the same scaling properties, i.e., that the moments of the corresponding distribution are everywhere proportional, up to a (moment-dependent) numerical constant. This assumption is a natural extension of the Kolmogorov refined similarity hypothesis [11].

(ii) Moment hierarchy:

$$\frac{\langle \pi_l^{p+1} \rangle}{\langle \pi_l^p \rangle} = A_p \left[\frac{\langle \pi_l^p \rangle}{\langle \pi_l^{p-1} \rangle} \right]^{\beta} , \quad 0 \le \beta \le 1 , \tag{7}$$

where A_p are numerical constant. Note that the condition $\beta \le 1$ guarantees convergence of all the moments, since (7) implies that

$$\langle \pi_l^p \rangle \propto \langle \pi_l \rangle^{(1-\beta^p)/(1-\beta)} . \tag{8}$$

Note also that it means that $\epsilon_l^{(\infty)} \sim \langle \pi_l \rangle^{-\beta^p} \langle \epsilon_l^{p+1} \rangle / \langle \epsilon_l^p \rangle$ for all p, so that if $\beta < 1$ we have exactly

$$\epsilon_l^{(\infty)} \sim \lim_{p \to \infty} \frac{\langle \epsilon_l^{p+1} \rangle}{\langle \epsilon_l^p \rangle} . \tag{9}$$

The normalization factor $\epsilon_l^{(\infty)}$ can then be interpreted as tracing the tail of the most intermittent structures.

(iii) Power-law intermittency:

$$\langle \pi_l \rangle \sim \left[\frac{\langle \delta v_l^3 \rangle}{\epsilon_0 l_K} \right]^{\Delta} , \tag{10}$$

where l_K is the Kolmogorov scale. This assumption merely states that the dissipative structures are spatially intermittent [4].

The combination of the three assumptions implies that the structure functions follow the extended self-similarity:

$$\langle \delta v_l^p \rangle = C_p \langle \delta v_l^3 \rangle^{\tilde{\zeta}_p} , \tag{11}$$

with a relative exponent:

$$\tilde{\zeta}_p = (1-\Delta)\frac{p}{3} + \Delta \frac{(1-\beta^{p/3})}{(1-\beta)} . \tag{12}$$

The scaling of the structure functions in the inertial range $\langle \delta v_l^p \rangle \sim l^{\zeta_p}$ corresponds then simply to an absolute scaling exponent:

$$\zeta_p = \zeta_3 \tilde{\zeta}_p . \tag{13}$$

Taking $\zeta_3 = 1$ and $\Delta = \beta = 2/3$, one finds the formula proposed by She and Léveque [5], which fits very well the experimental data on fully developed isotropic 3D turbulence. The nonintermittent K41 model is obtained with $\beta = 1$ and/or $\Delta = 0$. An interesting observation is that the value of $\tilde{\zeta}_p$ depends only on the scaling properties of $\langle \epsilon_l \rangle / \epsilon_l^{(\infty)}$ as a function of $\langle \delta v_l^3 \rangle$. In other words, one could get the same relative exponent whether $\langle \epsilon_l \rangle$ is scale independent or not, as long as the ratio $\langle \epsilon_l \rangle / \epsilon_l^{(\infty)}$ keeps the scaling.

B. Adaptation of the theory to 2D turbulence

Some adaptation is needed to apply SL theory to 2D turbulence. Here we consider the situation in which a two-dimensional incompressible turbulence is forced by a stationary force whose spectrum is concentrated in a neighborhood of the wave number k_I and in which a statically steady state is reached. Therefore, the mean kinetic energy $E(t) = \langle |\vec{v}(\vec{x},t)|^2 \rangle / 2$ and the enstrophy

$Z(t)=\langle \omega(\vec{x},t)^2\rangle/2$ remain constant in time. Here, $\vec{v}$ is the velocity, $\omega=\mathrm{curl}\vec{v}$, and $\langle\ \rangle$ refers to averaging over all the position vector $\vec{x}$. The velocity field is then determined by 2D vorticity equation

$$\partial_t\omega+J(\omega,\psi)=F+\nu\Delta\omega\ , \tag{14}$$

where ψ is the stream function, J the two-dimensional Jacobian, and F the forcing. It is well known that in the decaying inviscide case as well as in a statistically steady state, corresponding to the compensation of the energy input by the dissipation at large and small scales, the 2D vorticity equation (14) is characterized by a family of integral constraints very different from the 3D situation. The particular quadratic invariants are in this case the kinetic energy and the enstrophy which are transferred via nonlinear term in (14) from one scale to another, following Kolmogorov's cascade scenario: a direct enstrophy cascade from injection scales $l_I\sim k_I^{-1}$ toward small scales where viscous dissipation acts, and an inverse energy cascade always towards large scales. Since viscous dissipation is negligible in the limit of small k, we assume that a statistically steady state is maintained by the friction effect of the external fields. In this situation, all numerical simulations in periodic domain (see, e.g., [2,3,12]) show a spontaneous appearance of high vorticity concentrations inside persistent coherent vortices having approximately the same characteristic size $l_I=\pi k_I^{-1}$. These vortices induce basic space-time inhomogeneities of the 2D turbulent dynamics.

As in 3D turbulence, we shall consider the scaling of the structure functions of the velocity differences, $\langle \delta v_l^p\rangle$. Following the ESS hypothesis, we shall specifically consider the relative scaling of the structure function, as a function of the scale:

$$\langle \delta v_l^p\rangle\sim\langle \delta v_l^3\rangle^{\tilde{\zeta}_p}\ . \tag{15}$$

We shall investigate the existence of different regimes for $\tilde{\zeta}_p$, corresponding to the different spectral regimes (inverse energy cascade, coherent structures, enstrophy cascade).

Because of the enstrophy cascade at small scales and the energy cascade at large scales, it is clear that the refined similarity hypothesis (6) has to be modified. As stressed by Kraichnan [13,14], a truly inertial range quantity is given by fluxes of a given quantity, rather than dissipation of the quantity. These considerations lead us to define the nondimensional quantity π_l appearing in (5) in terms of the transfer produced by the nonlinear term in (14), η_l:

$$\eta_l=\frac{1}{l}\int_l|\omega(v\cdot\nabla)\omega\,dr|\ . \tag{16}$$

Therefore

$$\pi_l=\frac{\eta_l}{\eta_l^\infty}\ , \tag{17}$$

with

$$\eta_l^\infty=\lim_{p\to\infty}\frac{\langle\eta_l^{p+1}\rangle}{\langle\eta_l^p\rangle}\ , \tag{18}$$

The nondimensional quantity π_l is clearly directly related to the cascade dynamics.

We assume that the three hypotheses formulated in Sec. II A are still satisfied in terms of this new nondimensional quantity. This means that formula (12) characterizing the *relative* scaling exponent $\tilde{\zeta}_p$ is in some sense universal, and valid for both 2D and 3D turbulence. The difference between these two cases only enters in the value of the *absolute* scaling exponent $\zeta_p=\zeta_3\tilde{\zeta}_p$ via the value of ζ_3, which is, respectively, 1 for 3D and 2D energy cascade and the 3 for 2D enstrophy cascade. The advantage of using the relative scaling exponent is that it is a simple measure of intermittency: if the (energy or enstrophy) cascade is not intermittent, then $\tilde{\zeta}_p=p/3$, corresponding to $\Delta=0$ or $\beta=1$. If the cascade is intermittent, the relative scaling exponent should then follow (12), with parameters Δ and β possibly different in the enstrophy and energy range, characterized by different conservation laws (see Dubrulle [4]).

C. The numerical 2D simulations

We use classical Eulerian simulations of stationary forced and dissipate incompressible two-dimensional turbulence which solve the vorticity equation (14) in the form

$$\partial_t\omega+J(\omega,\psi)=F+D_\omega+D_\epsilon \tag{19}$$

on a periodic square domain $(2\pi,2\pi)$, using a pseudospectral scheme. The forcing F is defined by keeping constant in time the amplitude of the zonal mode $(0,k_I)$; the term D_ω represents the dissipation of enstrophy at the largest resolved wave number $k\sim\pi l_c^{-1}$, where l_c is the cutoff scale; D_ϵ represents a linear friction at the largest scales ($k\sim\pi l_d^{-1}$, where l_d is the scale corresponding to the system size). $D_\epsilon=t_d^{-1}l_d^{-2}\psi$, t_d is a characteristic friction time. The numerical integration was pursued long enough to reach a stationary regime in which energy and enstrophy spectra do not vary in time. This corresponds to the equilibrium state when the mean energy and enstrophy input is compensated by the mean dissipation rate at large and small scales. Consequently, our simulations do not describe the phenomena of Bose condensation due the presence of finite boundaries [15]

In the sequel, we shall consider three different simulations, referred to, respectively, as R1024F256, R1024F10, and R1728F40.

R1024F256 is a simulation with a resolution 1024×1024, and a forcing at a large wave number $k_I=256$. This simulation therefore presents a well-developed inverse cascade of energy. The dissipation used in this simulation is parametrized by the anticipated potential vorticity method (APVM) [16]:

$$D_\omega=J[\psi,\theta(-l_c^2\nabla^2)^4J(\psi,\omega)]\ , \tag{20}$$

where θ is a characteristic dissipation time scale. The scheme APVM was introduced by Sadourny and Basdevant [17,18] for the barotropic vorticity equation to efficiently parameterize the subgrid scales flux. One of its advantages compared to the hyperviscosity method is

that it produces a realistic amplitude of the large-scale barotropic modes when the cutoff scale is of the order of the input scale.

R1024F10 is a simulation with resolution 1024×1024, and a forcing at small wave number $k_I=10$. This simulation presents a well-developed direct cascade of enstrophy.

R1728F40 is a high-resolution simulation 1728×1728, with a forcing at the wave number $k_I=40$. In this simulation, both the inverse cascade of energy and the direct cascade of enstrophy can be studied.

The dissipation at largest resolved wave number used in two later simulations is parametrized by the hyperviscosity method:

$$D_\omega=-t_c^{-1}(-l_c^2\nabla^2)^8\omega\ , \tag{21}$$

where t_c is another characteristic time scale.

We would like to emphasize that contrary to recently performed numerical experiments by Borue [19] and Smith and Yakhot [15], we use in all our simulations a linear friction at largest scales. The other difference consists in the parametrization of the subgrid scales flux when the cutoff is of the order of the forcing scale (experiment R1024F256). In this case, we utilize (20) [and not the usual (21)] while in [19] and [15] the subgrid scales flux is parametrized by (21).

The energy spectra and energy and enstrophy fluxes for R1024F256 and R1728F40 are displayed, respectively, in Figs. 1 and Fig. 2 as a function of the wave number k. $l_I=\pi/k_I$ and $l_E=\pi/k_E$ are, respectively, the forcing and the most energetic scales. The energy range is characterized by wave numbers $k_E<k<k_I$, the enstrophy range by wave numbers $k>k_I$. Our three simulations confirm previously reported results [20,21]: in the energy range, we observe a $k^{-5/3}$ spectrum characteristic of the inverse cascade of energy predicted by Kraichnan [13]; in the enstrophy range, for $k\gg k_I$, we observe up to wave number k_D a $k^{-3.5}$ spectrum, steeper than the theoretical k^{-3} prediction. In the two cases where the enstrophy cascade is sufficiently developed (R1024F10 and R1728R40), we may note the existence of a range of scale, extending beyond k_I towards larger wave numbers, where the spectra do not follow a well-defined scaling. We shall label the end of the corresponding range of scale by k_{CS}. This range scale ($k_I<k<k_{CS}$) has been previously identified [2] as corresponding to the strong coherent structures observed in forced 2D simulations. The absence of spectral scaling in the range of scale corresponding to the coherent structure can be seen as the manifestation of the "laminar" character of these structures [1]. As we shall see, other manifestations of this "laminar" character will appear when considering other scaling properties.

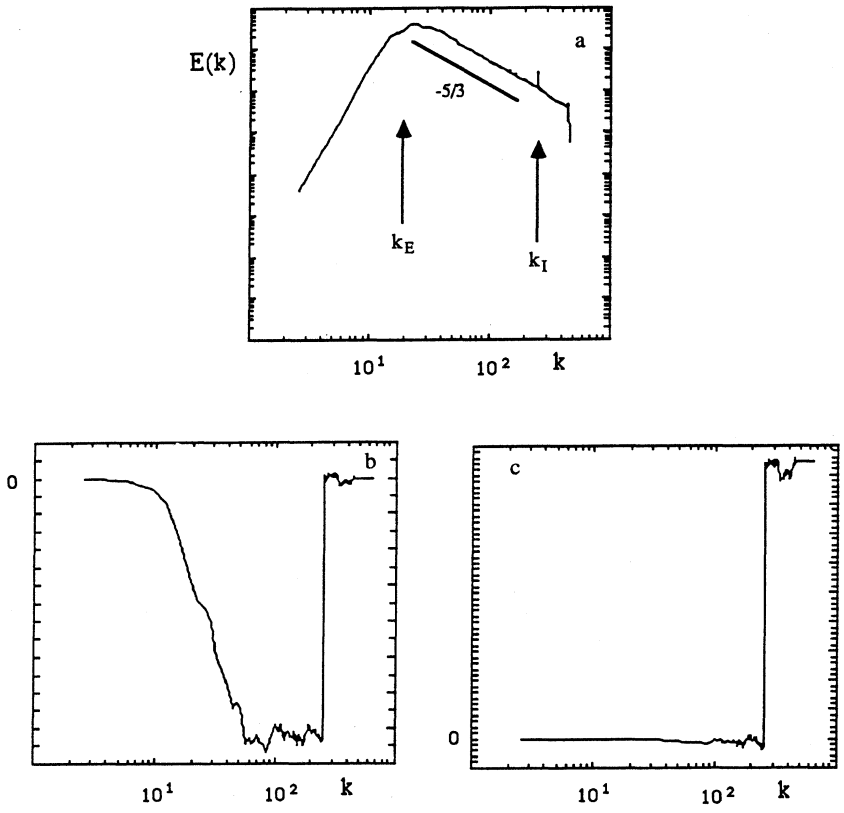

FIG. 1. Energy spectra (a), energy (b), and enstrophy fluxes (c) as a function of wave number k. Arrows indicate the injection wave number k_I and the most energetic wave number k_E; the resolution used is 1024×1024 (log-log scale).

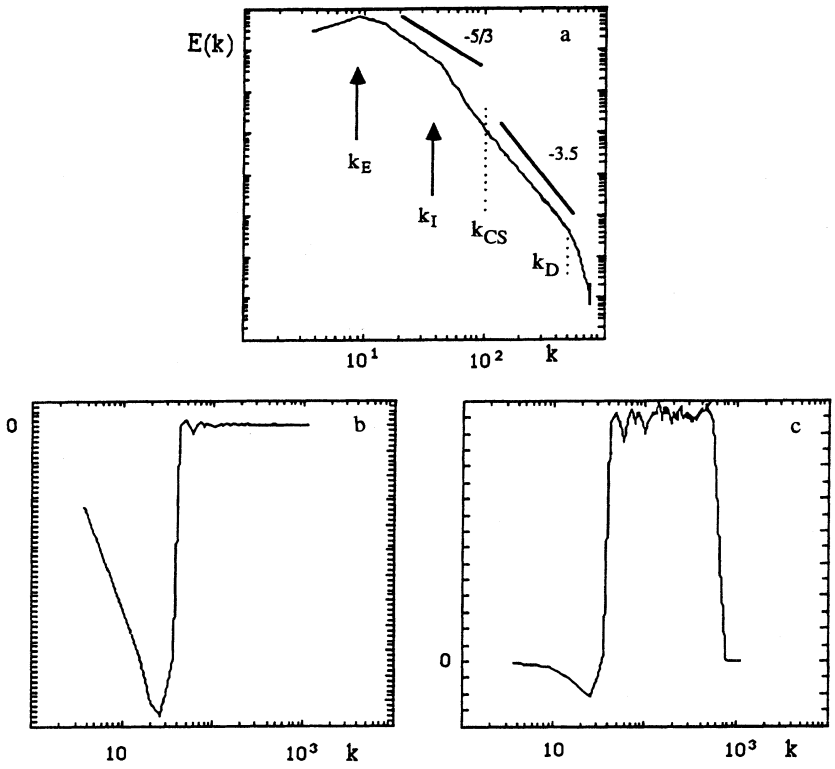

FIG. 2. Energy spectra (a), energy (b), and enstrophy fluxes (c) as a function of wave number k. Arrows indicate the injection wave number k_I, the most energetic wave number k_E, as well as k_{CS} and k_D; the resolution is 1728×1728 (log-log scale).

III. RESULTS

A. Structure functions

The velocity structure function $\langle \delta v_l^p \rangle$ as a function of the nondimensional scale separation $l = k_I k^{-1}$ (where k_I is the injection wave number) have been computed for $p = 2$, 3 4, 6, 8, 10, and 12 in the case R1024F256 [Fig. 3(a)] and R1728F40 [Fig. 4(a)]. In the first case [corresponding to the inverse energy cascade, Fig. 3(a)], one may note an approximate scaling range between k_I and k_E, followed by a large-scale saturation, where all the structure functions become independent on the scale. In the second case [the enstrophy cascade, Fig. 4(a)], one observes a well-defined scaling regime below k_{CS}, a large-scale saturation after k_I, and an intermediate regime between k_{CS} and k_I, where the scaling is contaminated by the existence of a bump at k_I. The same structure functions have been plotted also following the ESS representation (2), as a function of the third structure function ($s = 3$) in Fig. 3(b) (for R1024F256) and Fig. 4(b) (for R1728F40). One may note a clear improvement of the scaling regime between k_I and k_E in the inverse energy cascade, but no noticeable improvement in the enstrophy cascade case, especially in the domain of the coherent structure. Thus, it seems that coherent structure somehow prevents the development of ESS, which would suggest that it is a phenomenon associated with strongly turbulent motions.

The scaling exponents of the structure functions have also been estimated. From comparison between Fig. 5(a) (exact local exponent as a function of scale) and Fig. 5(b) (relative local exponent computed using ESS), it is clear that the relative scaling exponents are much better defined than the exact exponents in the inverse energy cascade, and extend within at least a decade of wave number. Note also the progressive deterioration of the estimation for $p > 6$, due to a lack of statistics. In the enstrophy cascade range, one may note that even the relative scaling exponents are not well defined in the coherent structure range, in contrast with both exact and relative exponents at smaller scales. The measured values of the relative scaling exponents $\tilde{\zeta}_p^{\text{meas}}$ in the range where they are well defined have been reported in Tables I–IV for all our experiments. The values measured in the enstrophy cascade, although rather inaccurate, are very close to the linear K41 law ($\tilde{\zeta}_p = p/3$). This is in agreement with both Kraichnan [13,14] and the Lebedev and Falkovich model [22,23], which predicts no intermittency in the enstrophy cascade.

B. Definition of π_l

The check of the various hypotheses described in Sec. II requires that the quantity π_l appearing in (17) is well defined, i.e., that the quantity $S_p(l) = \langle \eta_l^{p+1} \rangle / \langle \eta_l^p \rangle$ converges to a finite limit. Figure 6 shows S_p as a function of $\langle |\delta v_l|^3 \rangle$ for increasing values of p (up to $p = 15$). One indeed observes a saturation of this quantity towards large values of p. In practice, we therefore adopted $S_{15}(l)$ as an estimation of η_l^∞ to compute π_l according to (17).

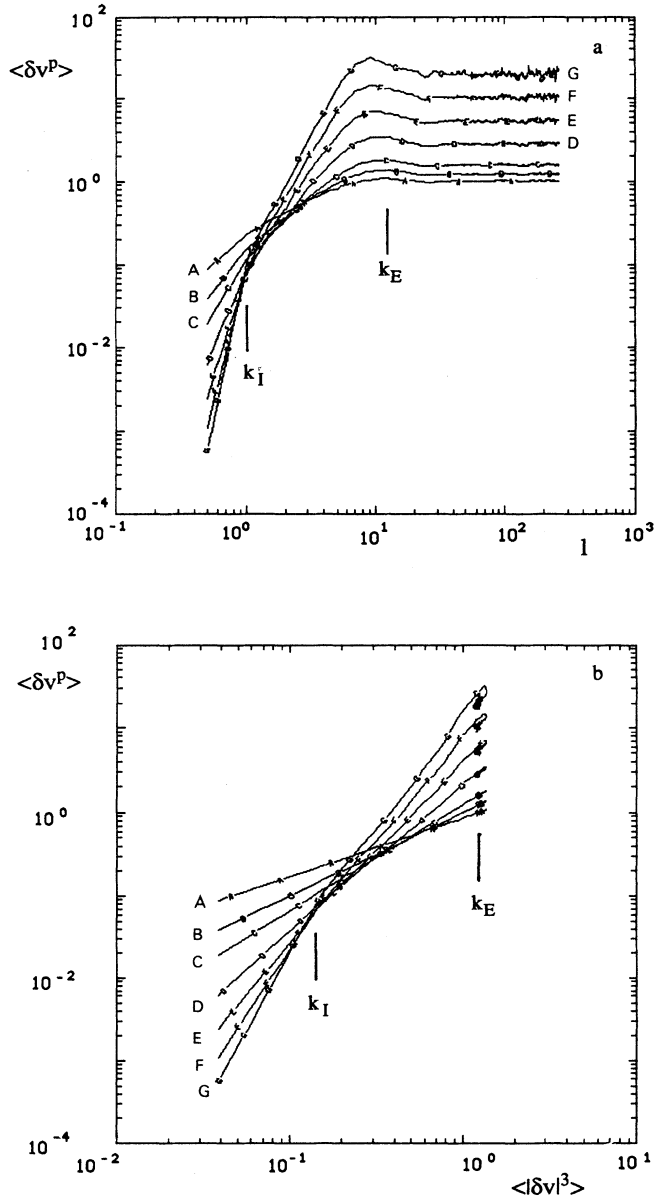

FIG. 3. Velocity structure functions $\langle \delta v^p \rangle$ as a function of (a) the nondimensional scale l and (b) $\langle |\delta v|^3 \rangle$ for $p=2$ (A), 3 (B), 4 (C), 6 (D), 8 (E), 10 (F), and 12 (G); scales corresponding to k_I and k_E are indicated. Experiments R1024F256 (log-log scale).

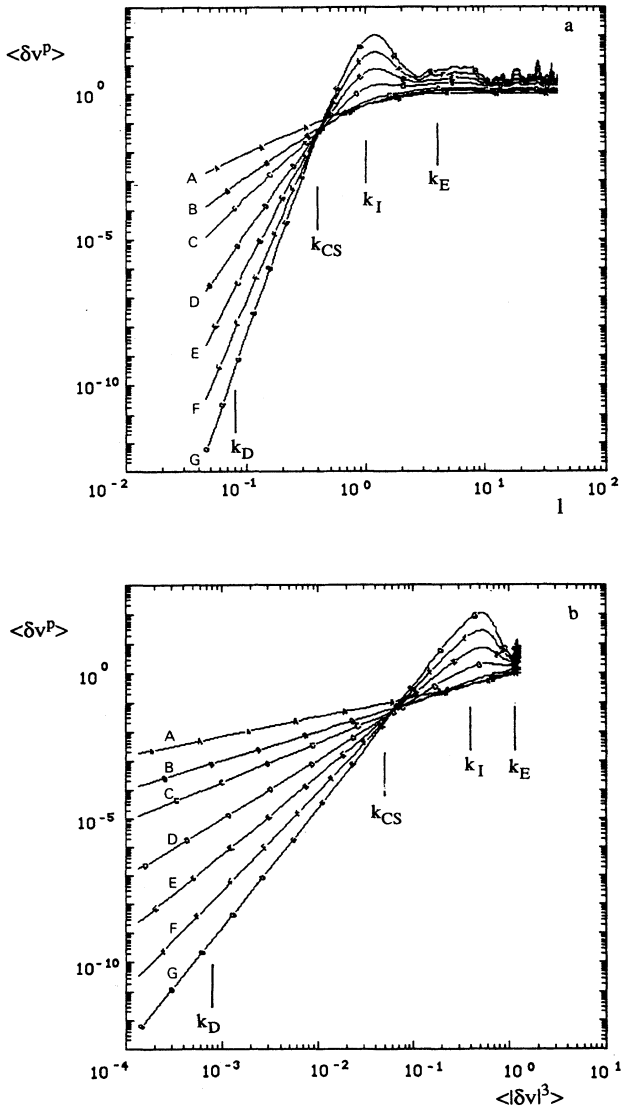

FIG. 4. Velocity structure functions $\langle \delta v^p \rangle$ as a function of (a) the nondimensional scale l and (b) $\langle |\delta v|^3 \rangle$ for $p=2$ (A), 3 (B), 4 (C), 6 (D), 8 (E), 10 (F), and 12 (G); scales corresponding to k_I, k_E, k_{CS}, and k_D are indicated. Experiment R1728F40 (log-log scale).

C. Refined similarity hypothesis

A test of the refined similarity hypothesis (6) can be made by the following procedure. By definition of π_l, we have

$$\frac{\langle \pi_l^p \rangle}{\langle \pi_l \rangle^p} = \frac{\langle \eta_l^p \rangle}{\langle \eta_l \rangle^p} \ . \tag{22}$$

If we assume $\langle \eta_l^p \rangle$ to obey some scaling property in some well-defined range, $\langle \eta_l^p \rangle \sim l^{\tau_p}$, we should then have

$$\frac{\langle \pi_l^p \rangle}{\langle \pi_l \rangle^p} \sim \langle \delta v_l^3 \rangle^{\gamma_p} \ , \tag{23}$$

with $\gamma_p = (\tau_p - p\tau_1)/\zeta_3$. The refined similarity hypothesis will then be satisfied if

$$\zeta_p = \frac{p}{3} + \gamma_{p/3} \ . \tag{24}$$

Our test of the refined similarity hypothesis consists then first in computing $\gamma_{p/3}$ using Eq. (23), and then checking that (24) is satisfied. Note that $\gamma_{p/3}$ is a measure of the intermittency ($\gamma_{p/3}=0$ in the nonintermittent case).

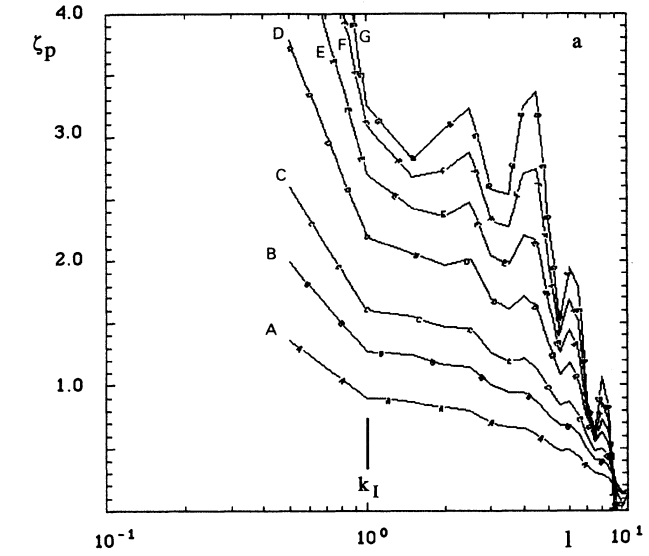

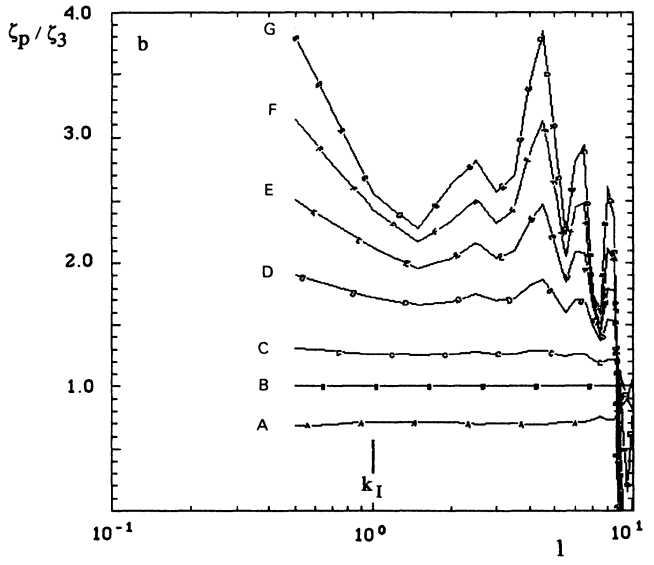

FIG. 5. (a) Absolute scaling exponent ζ_p and (b) relative scaling exponent $\tilde{\zeta}_p$ as a function of the nondimensional scale l. Experiment R1024F256 (lin-log scale).

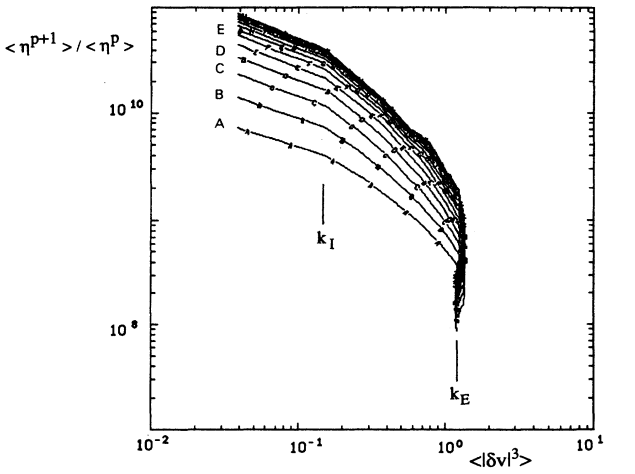

FIG. 6. The quantity $S_p = \langle \eta_{p+1} \rangle / \langle \eta_p \rangle$ as a function of $\langle |\delta v|^3 \rangle$ for increasing values of p ($p \leq 15$). Experiment R1024F256 (log-log scale).

Note that the measurement of $\gamma_{p/3}$ can be expected to be more accurate than the measurement of $\tilde{\zeta}_p$, because it involves lower moments (or order $p/3$ rather than p). Figures 7(a) and 7(b) show $\langle \pi_l^{p/3} \rangle / \langle \pi_l \rangle^{p/3}$ as a function of $\langle \delta v_l^3 \rangle$ for, respectively, R1024F256 and R1728F40. One observes well-defined scaling laws, which enable accurate determination of the exponent $\gamma_{p/3}$. The corresponding values are given in Tables I and II, together with the check of (24). It can be seen that the refined similarity hypothesis is reasonably well satisfied. Since the computation of $\gamma_{p/3}$ is more accurate, from now on we may accept $p/3 + \gamma_{p/3}$ as an estimation of $\tilde{\zeta}_p$, rather than the value directly measured, using structure functions. One may then note that the intermittency (deviation from the Kolmogorov law $\tilde{\zeta}_p = p/3$) is much stronger in the inverse cascade than in the enstrophy cascade. Actually, the values derived in the inverse energy cascade are close to those measured in 3D isotropic turbulence [8]. The same check was also performed on the run R1024F10, in which the intermittency in the enstrophy cascade was found slightly stronger than in R1728F40. The results are reported in Table III.

D. Moment hierarchy

The moment hierarchy (7) can be tested directly by plotting $R_p(l) = \langle \pi_l^{p+1} \rangle / \langle \pi_l^p \rangle$ as a function of $R_{p-1}(l)$ for different p. This is done in Fig. 8 for both R1024F256 (filled circles) and R1024F10 (open circles). The lines connect values of $R_p(l)$ with the same index p. Only values of l lying, respectively, in the energy cascade range $k_E < k < k_I$ (for R1024F256) and in the enstrophy cascade range $k_{CS} < k < k_D$ for R1024F10 have been kept. If the hierarchy holds, all lines corresponding to different values of p should be parallel to each other, with a slope β. One may indeed note in Fig. 8 such a tendency, with clear evidence for different values of β for R1024F256 ($\beta = 0.7$) and R1024F10 ($\beta = 0.55$). The different lines are apparently all aligned, enabling a good determination of β in both cases. In the case R1728F40, the same procedure gives an estimate of β in the enstrophy cascade range much closer to 1 ($\beta = 0.75$). Estimate of β in the inverse cascade range could not be done accurately, because of the lack of resolution at these scales. The difference between the parameter β estimated in the run R1728F40 and R1024F10 might be interpreted in various ways. This could mean, for example, that β does not depend only on the conservations laws, as populated by Dubrulle [4], but also on the other parameters such as the

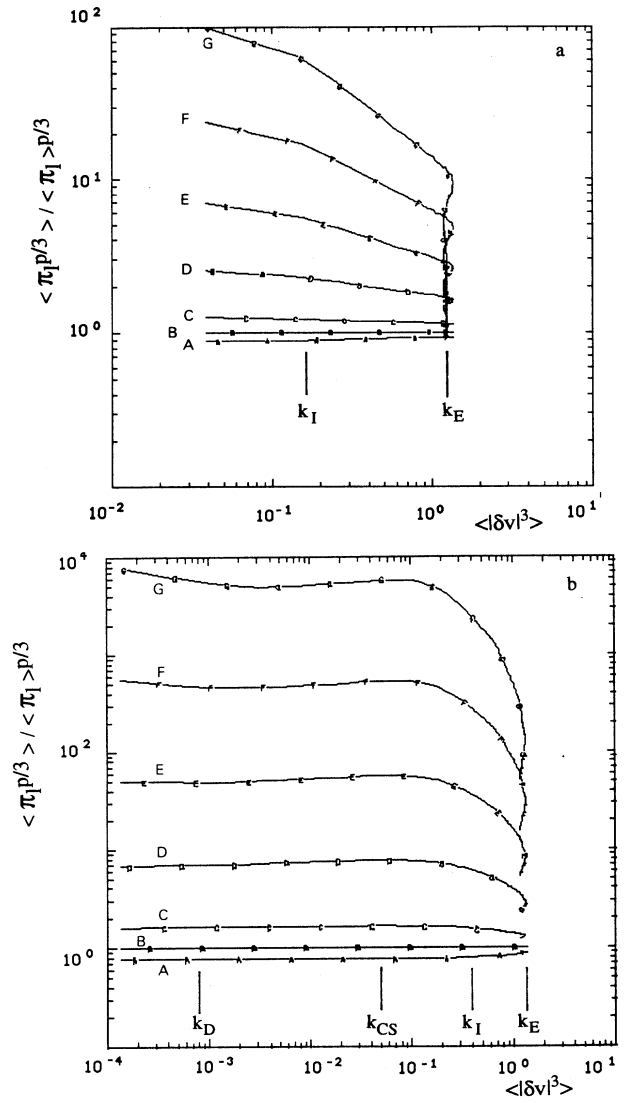

FIG. 7. The quantity $\langle \pi_l^{p/3} \rangle / \langle \pi_l \rangle^{p/3}$ as a function of $\langle |\delta v|^3 \rangle$ and definition of γ_p; (a) experiment R1024F256, (b) experiment R1728F40 (log-log scale).

Reynolds number. This could be due to the fact that R1024F10 does not fully include all the dynamics of 2D turbulence, because it does not resolve the inverse energy cascade. Finally, we may mention that there is a rather large inaccuracy in the determination of these exponents, becuase this representation does not enable us to disentangle lines corresponding to $p > 3$, which all scatter near the $R_p(l)=1$ range. We thus tried another representation, in which $\langle \pi_l^{p/3} \rangle$ is plotted as a function of $\langle \pi_l \rangle$. If the hierarchy holds, one should obtain straight lines, with slope $(1-\beta^{p/3})/(1-\beta)$ [see Eq. (8)]. If $\beta < 1$, one may expect a saturation in the slopes for large p, towards the value $1/(1-\beta)$. The results are shown in Fig. 9(a) (for R1024F256) and Fig. 9(b) (for R1024F10). In the latter case, one may note a bump developing in the range where

TABLE I. Scaling exponents of the run R1024F256 in the inverse energy cascade range $k_E \le k \le k_I$. ζ_p is the relative scaling exponent of the velocity structure function; $\gamma_{p/3}$ is the relative scaling exponent of the enstrophy flux; if the refined self-similarity hypothesis is valid, one should have $\zeta_p = p/3 + \gamma_{p/3}$; Δ is the intermittency exponent; "meas" and "th" refer, respectively, to measured and theoretical values. The theoretical values have been computed using the SL formula, with $\Delta = 0.47$ and $\beta = 0.7$.

p	ζ_p^{meas}	$\gamma_{p/3}$	$p/3+\gamma_{p/3}$	ζ_p^{th}
2	0.7±0.01	0.016±0.001	0.68	0.68
4	1.27±0.01	−0.033±0.001	1.3	1.30
6	1.73±0.03	−0.144±0.001	1.86	1.86
8		−0.32±0.002	2.35	2.37
10		−0.53±0.02	2.8	2.86
12		−0.8±0.05	3.2	3.31

TABLE II. Scaling exponents of the run R1728F40 in the inverse energy cascade range $k_E \le k \le k_I$. ζ_p is the relative scaling exponent of the velocity structure function; $\gamma_{p/3}$ is the relative scaling exponent of the enstrophy flux; if the refined self-similarity hypothesis is valid, one should have $\zeta_p = p/3 + \gamma_{p/3}$; Δ is the intermittency exponent; "meas" and "th" refer, respectively, to measured and theoretical values. The theoretical values have been computed using the SL formula, with $\Delta = 0.4$ and $\beta = 0.35$.

p	ζ_p^{meas}	$\gamma_{p/3}$	$p/3+\gamma_{p/3}$	ζ_p^{th}
2	0.8±0.01	0.06±0.002	0.72	0.71
4	1.0±0.05	−0.1±0.02	1.23	1.26
6		−0.4±0.03	1.6	1.74
8		−0.7±0.06	1.97	2.18
10		−0.9±0.07	2.43	2.6
12		−1.2±0.09	2.8	3.01

TABLE III. Scaling exponents of the run R1024F10 in the enstrophy cascade range $k_{CS} \le k \le k_D$. ζ_p is the relative scaling exponent of the velocity structure function; $\gamma_{p/3}$ is the relative scaling exponent of the enstrophy flux; if the refined self-similarity hypothesis is valid, one should have $\zeta_p = p/3 + \gamma_{p/3}$; Δ is the intermittency exponent; "meas" and "th" refer, respectively, to measured and theoretical values. The theoretical values have been computed using the SL formula, with $\Delta = 0.13$ and $\beta = 0.55$.

p	ζ_p^{meas}	$\gamma_{p/3}$	$p/3+\gamma_{p/3}$	ζ_p^{th}
2	0.66±0.01	0.0±0.002	0.66	0.67
4	1.34±0.01	0.0±0.002	1.33	1.32
6	2.02±0.02	−0.02±0.01	1.98	1.94
8		−0.12±0.01	2.56	2.55
10		−0.23±0.02	3.13	3.15
12		−0.35±0.05	3.65	3.74

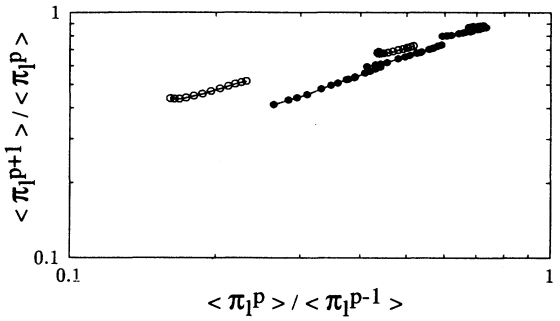

FIG. 8. The moment hierarchy and definition of β; black circles, experiment 1024F256; white circles, experiment R1024F10 (log-log scale).

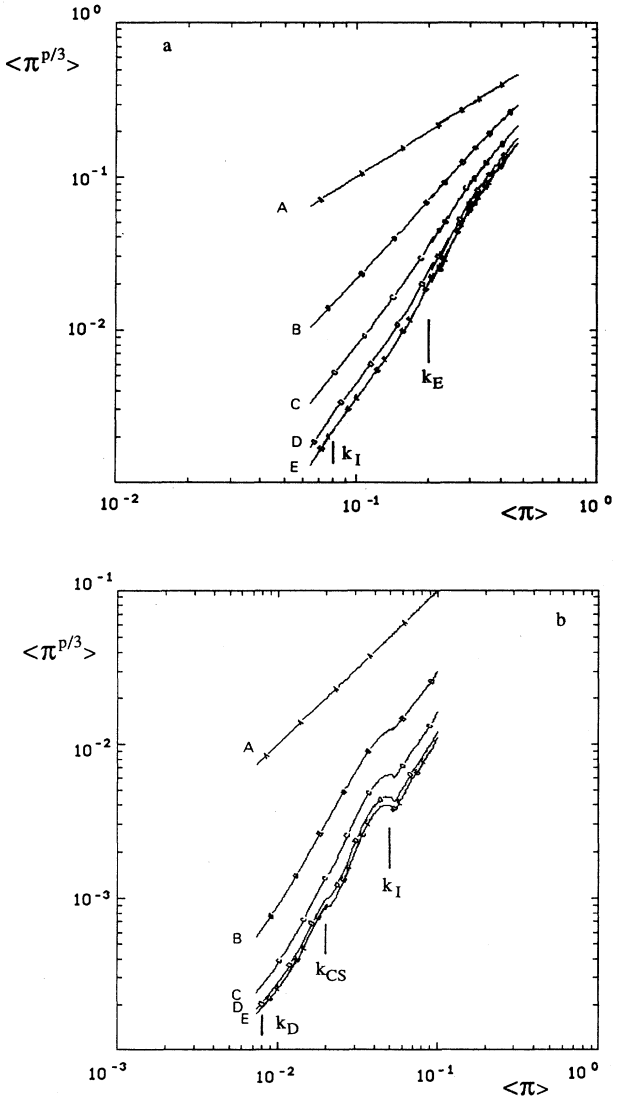

FIG. 9. Definition of β using relation (8); (a) experiment R1024F256, (b) experiment R10324F10 (log-log scale).

coherent structure dominates, resulting in a deterioration and a loss of the scaling. This shows that the moment hierarchy is incompatible with the presence of coherent structures. In the range of scale where the scaling is well defined, we may compute the values of β for different p, assuming that the slope is $(1-\beta^{p/3})/(1-\beta)$. For R1024F256, we find β decreasing from $\beta=0.71$ for $p=6$, down to $\beta=0.56$ for $p=15$. For R1024F10, we find $\beta=0.75$ for $p=6$ and $\beta=0.44$ for $p=15$. These values are compatible with the values obtained using the first method, but imply rather large error bars on the determination of β. This allows us to reconcile somehow the difference in values of β found in the runs R1024F10 and R1728F40 using the first method. We cannot, however, rule out the possibility that β is not constant in the hierarchy, and may vary with p, up to an asymptotic value. As we shall see, however, the value of β obtained using the first method enables a good fit of the exponents of the structure function using the SL formula. This argument is in favor of a single value of β throughout the hierarchy.

E. Scaling intermittency

To check the third hypothesis (10) and determine the scaling exponent Δ (if it exists), we have made plots of $\langle \pi_l \rangle_p \equiv \langle \eta_l \rangle \langle \eta_l^p \rangle / \langle \eta_l^{p+1} \rangle$ as a function of $\langle \delta v_l^3 \rangle$. The results are shown in Fig. 10(a) (for R1024F256) and Fig. 10(b) (for R1024F10). In the limit $p \to \infty$, $\langle \pi_l \rangle_p$ tends to $\langle \pi_l \rangle$ defined in (17). Therefore, if the third hypothesis is valid, $\langle \pi_l \rangle_p$ should behave as $\langle \delta v_l^3 \rangle^{\Delta}$ for large enough p. Figures 10(a) and 10(b) indeed show a saturation of the quantity $\langle \pi_l \rangle_p$ for $p > 10$, with scaling properties in some range of scales. For R1024F256 (the inverse energy cascade run), a well-defined scaling law holds in a range corresponding to $k_E < k < k_I$, with exponent $\Delta=0.47$. For R1024F10, the scaling holds only in part of the scale range $k_{CS} < k < k_D$, because of a "bump" occurring near $k = k_{CS}$. This is not consistent with the scaling properties of other quantities, which were found to hold in the whole range $k_{CS} < k < k_D$. This somehow casts doubt on the generality of the third hypothesis and its applicability when coherent structures are present in the flow. Nevertheless, if one estimates the exponent Δ in the limited range of scale where it exists, one finds $\Delta=0.13$, much lower than in the inverse energy cascade.

F. Validity of SL formula

As a last consistency check, we computed the theoretical relative scaling exponents ζ_p^{th} using SL formula (12) and the values of β and Δ found in the preceding sections. The results are given in Tables I–IV. One may compare these estimates with the measured value $\zeta_p^{\text{meas}} = p/3 + \gamma_{p/3}$ (see Sec. III C). The agreement is quite good for R1024F256, but less satisfactory (although reasonable) for R1024F10. This may be partly due to the fact that the scaling properties were not rigorously satisfied in the enstrophy cascade range, because of the influence of coherent structures.

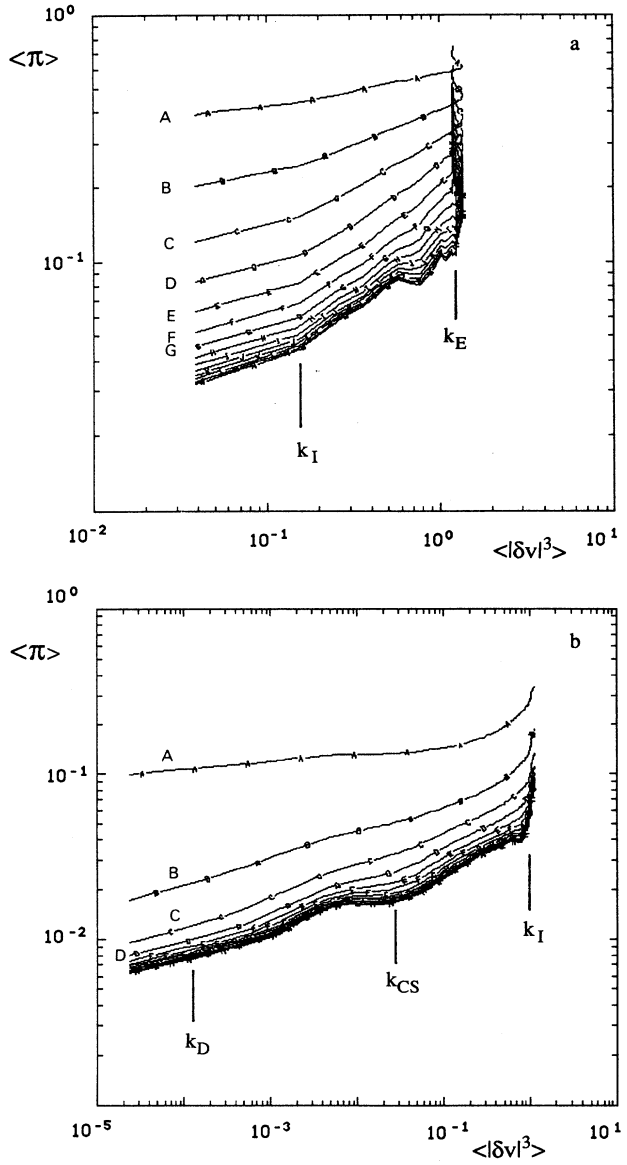

FIG. 10. Quantity $\langle \pi_l \rangle$ as a function of $\langle |\delta v|^3 \rangle$ and definition of the scaling exponent Δ using relation (10); (a) experiment R1024F256, (b) experiment R1024F10 (log-log scale).

TABLE IV. Scaling exponents of the run R1728F40 in the direct enstrophy cascade range $k_{CS} \leq k \leq k_D$. ζ_p is the relative scaling exponent of the velocity structure function; $\gamma_{p/3}$ is the relative exponent of the enstrophy flux; if the refined self-similarity hypothesis is valid, one should have $\zeta_p = p/3 + \gamma_{p/3}$; Δ is the intermittency exponent; "meas" and "th" refer, respectively, to measured and theoretical values. The theoretical values have been computed using the SL formula, with $\Delta = 0$ and $\beta = 0.8$

p	ζ_p^{meas}	$\gamma_{p/3}$	$p/3+\gamma_{p/3}$	ζ_p^{th}
2	0.66±0.004	0.0±0.002	0.66	0.66
4	1.34±0.01	0.0±0.05	1.34	1.33
6	2.04±0.02	−0.02±0.01	2.02	2.00
8	2.75±0.05	−0.03±0.01	2.69	2.66
10	3.45±0.05	−0.05±0.02	3.38	3.33
12	4.1±0.1	−0.05±0.03	4.05	4.00

IV. DISCUSSION

We begin by summarizing the main results. Our study of scaling properties of velocity structure functions in high-resolution numerical simulation of stationary 2D turbulence has revealed that the direct cascade of enstrophy is characterized by a very weak intermittency, while the inverse cascade of energy displays an intermittency with corrections similar to that found in 3D turbulence. We would like to note that the latter result is restricted to the cases of stationary turbulence and perhaps can be extended neither to decaying turbulence nor to the case of inverse energy cascade in the presence of Bose condensation, considered by Smith and Yakhot [13]. Following these authors, the intermittency in the inverse cascade range appears only in the presence of Bose condensation at the largest scales.

The two "domains of intermittency" are separated in the scale space by a domain in which coherent structures dominate the dynamics, and in which no scaling property can be detected. The intermittency corrections found in the two scaling regimes were compared with a prediction given by a model from She and Lévêque [5] and Dubrulle [4]. The three main hypotheses pertaining to the prediction were checked independently and found to be reasonably well satisfied in the scaling regimes, proving that at least the theoretical prediction is a fair approximation to reality. The two main parameters of the theory β and Δ, connected, respectively, to the relation between the different moments of transfer in inertial range and to the structure of the highest moments, were estimated. In the energy cascade, values similar to those found in 3D turbulence were obtained. In the enstrophy cascade, Δ was found to be very small, consistent with the weak intermittency observed. As for β, it was found to vary between 0.5 and 1, depending on the resolution and the degree of development of the cascade.

We now examine some implications of the present results. The weak degree of intermittency observed in the enstrophy cascade shows that it cannot be held responsible for the corrections to the k^{-3} spectra often reported in numerical simulations. This confirms previous conjecture that these corrections are mainly due to the strong coherent structures, which were found in our analysis to display no special scaling properties. This somehow brings up again the question of the role of the coherent structures in corrections to exact Kolmogorov-like scaling, already addressed in 3D turbulence by Procaccia and Constantin [24]. Also, the absence of scaling properties found in the domain of coherent structure makes more plausible the hypotheses made by Benzi *et al.* [1], namely that they behave like "laminar drop embedded in a turbulent flow." Regarding the issue of universality, addressed in the Introduction, our results do not provide a definite answer, due to the impossibility of getting very

high-precision results. In this sense, we cannot say that a universality suggested by She-Lévêque-Dubrulle is more plausible than that advocated, for example, in statistical models of 2D turbulence [25] or in the model of "sweeping of the small eddies by the large one" by Falkovich and Lebedev [23]. The present work shows, however, the benefit of considering this possibility, and should be considered as an exploratory pioneering work that should be pursued and extended. This could possibly clarify some of the issues addressed in the course of this work, such as the constancy of β throughout the cascade or the dependence of β and Δ on the conservation laws or the viscosity. Some of these issues have already been addressed in certain theoretical work [26] or in numerical experiments performed on shell models of turbulence [8,27].

ACKNOWLEDGMENTS

This work was supported by a grant from the European Community (ERBCHRXCT920001), the French Government Program "Relance de l'Est," and Groupement de Recherche CNRS-IFREMER "Mécanique des Fluides Géophysiques et Astrophysiques." One of us (P.F.) acknowledges partial support from the Russian Found of Foundamental Investigation (Grant No. 94-01-00951-a). The numerical computation were performed under Contract No. 940338 of IDRIS.

[1] R. Benzi, G. Paladin, S. Patarnello, P. Santangelo, and A. Vulpiani, J. Phys. A Math. Gen. **19**, 3771 (1986).
[2] A. Babiano, C. Basdevant, B. Legras, and R. Sadourny, J. Fluid Mech., **183**, 379 (1987).
[3] P. Santangelo, R. Benzi, and B. Legras, Phys. Fluid A **1**, 1027 (1989).
[4] B. Dubrulle, Phys. Rev. Let. **73**, 959 (1994).
[5] Z. S. She and E. Lévêque, Phys. Rev. Lett. **72**, 336 (1994).
[6] Z. S. She and E. C. Waymire, Phy. Rev. Lett. **74**, 262 (1995).
[7] P. Frick, B. Dubrulle, and A. Babiano, Phys. Rev. E **51**, 5582 (1995).
[8] R. Benzi, S. Ciliberto, C. Baudet, G. Ruiz, and R. Tripiccione, Europhys. Lett. **24:4**, 275 (1993).
[9] A. Vincent and M. Meneguzzi, J. Fluid Mech. **225**, 1 (1991).
[10] F. Anselmet, Y. Gagne, E. J. Hopfinger, and R. A. Antonia, J. Fluid Mech. **140**, 63 (1984).
[11] A. N. Kolmogorov, Fluid Mech. **13**, 82 (1962).
[12] D. Elhmaidi, A. Provenzale, and A. Babiano, J. Fluid Mech. **251**, 533 (1993).
[13] R. H. Kraichnan, Phys. Fluid A **10**, 1417 (1967).
[14] R. H. Kraichnan, J. Fluid Mech. **47**, 525 (1971).
[15] L. M. Smith and V. Yakhot, Phys. Rev. Lett. **71**, 352 (1993).
[16] R. Sadourny and C. Basdevant, J. Atmos Sci. **42**, 1353 (1985).
[17] C. Basdevant and R. Sadourny, J. Mec. Pure Appl., special issue on two-dimensional turbulence, 495 (1984).
[18] C. Basdevant and R. Sadourny, CR. Acad. Sci. Paris **292**, 1061 (1981).
[19] V. Borue, Phys. Rev. Lett. **72**, 1475 (1994).
[20] U. Frisch and P-L. Sulem, J. Atmos. Sci. **42**, 1353 (1985).
[21] J. R. Herring and J. C. McWilliams, J. Fluid Mech. **153**, 229 (1985).
[22] G. Falkovich and V. Lebedev, Phys. Rev. E **49**, R1800 (1994).
[23] G. Falkovich and V. Lebedev Phys. Rev. E **50**, 3883 (1994).
[24] I. Procaccia and P. Constantin, Phys. Rev. Lett. **70**, 3416 (1993).
[25] R. Robert and J. Sommeria, Phys. Rev. Lett. **69**, 2776 (1992).
[26] B. Dubrulle and F. Graner (unpublished).
[27] R. Benzi, L. Kadanoff, D. Lohse, M. Mungan, and J. Wang (unpublished).